Catalysis Today 224 (2014) 77–82

Contents lists available at ScienceDirect

Catalysis Today

journal homepage: www.elsevier.com/locate/cattod

UV and visible light photoelectrocatalytic bactericidal performance of 100% {1 1 1} faceted rutile TiO_2 photoanode

Xiaolu Liu[a], Haimin Zhang[a], Chang Liu[b,**], Jiangyao Chen[a,c], Guiying Li[c], Taicheng An[c], Po-Keung Wong[d], Huijun Zhao[a,*]

[a] Centre for Clean Environment and Energy, Griffith University, Gold Coast Campus, QLD 4222, Australia
[b] College of Pharmacy, Liaoning Medical University, Jinzhou 121001, China
[c] State Key Laboratory of Organic Geochemistry, Guangzhou Institute of Geochemistry, Chinese Academy of Sciences, Guangzhou 510640, China
[d] School of Life Sciences, The Chinese University of Hong Kong, Shatin, NT, Hong Kong SAR, China

ARTICLE INFO

Article history:
Received 30 July 2013
Received in revised form
14 September 2013
Accepted 22 September 2013
Available online 23 October 2013

Keywords:
Rutile TiO_2
{1 1 1} facets
Photocatalysis
Photoelectrocatalysis
Inactivation

ABSTRACT

This work reported the use of a UV and visible light active rutile TiO_2 photoanode with 100% exposed {1 1 1} faceted surface for photocatalytic and photoelectrocatalytic bactericidal applications. The bactericidal performances of the photoanode with UV and visible light driven photocatalysis and photoelectrocatalysis processes were evaluated using *Escherichia coli* as the test bacteria. Under the UV irradiation, 99.97% inactivation of 45 mL of 1.0×10^7 CFU/mL *E. coli* cells can be achieved within 10 min for photoelectrocatalysis treatment, while only 96.40% inactivation can be obtained within 30 min for photocatalysis treatment. Under the visible light irritation, 88.46% inactivation can be achieved with 180 min photocatalytic treatment, while 100% inactivation by photoelectrocatalytic treatment can be achieved over the same period. The bactericidal performance of the rutile TiO_2 film was also evaluated for sunlight driven photocatalysis treatment. 1.0 mL of 1.0×10^7 CFU/mL *E. coli* cells can be completely inactivated within 2.0 min. The rutile TiO_2 film photocatalyst can be used for 20 consecutive bactericidal experiments without the noticeable change in bactericidal performance.

1. Introduction

As a class of superior photocatalysts, titanium dioxides (TiO_2) have been widely applied to environmental remediation [1–6]. Intensive studies have demonstrated that TiO_2 photocatalysis can be used to effectively and efficiently remove a wide spectrum of organic contaminants and inactivate microbial cells [5–12]. Since the pioneering work of Matsunaga et al., TiO_2 photocatalysis-based bactericidal techniques have been extensively reported [10,11,13]. To date, the anatase TiO_2 has been almost exclusively used for photocatalysis-based bactericidal applications [10,11,14–16], while the bactericidal applications of rutile TiO_2 are barely reported [17]. This is mainly due to that the conduction band edge potential of the rutile TiO_2 is ~0.2 V more positive than that of anatase TiO_2, resulting in a less efficient reduction half-reaction that often limits the overall photocatalytic efficiency [2,18–21]. However, such a drawback of rutile TiO_2 could be overcome by employing a photoelectrochemical technique [18–22]. With a photoelectrocatalytic system, the applied potential bias serves as an external driving force to timely remove the photocatalytically generated electrons to the external circuit then to the counter electrode where the reduction-half reaction takes place [18–22]. In such a way, the reduction half-reaction will never be the limiting step of the overall reaction [18–22]. Additional benefits of photoelectrocatalysis also include the enhanced catalytic activity resulting from the effectively suppressed charge recombination and prolonged lifetime of photoholes [18–22]. It is well-known that TiO_2 is a wide bandgap semiconductor (E_g = 3.2 and 3.0 eV for anatase and rutile, respectively), which is photoactive only under UV irradiation, incapable of utilizing sunlight to drive the photocatalytic process. To enable the sunlight driven photocatalytic process, doping and sensitization approaches are commonly used to improve the visible light activity of TiO_2-based photocatalysts [16,23–27]. The high photocorrosion resistance and superior stability are the intrinsic advantages of TiO_2-based photocatalysts. Although the above doping and sensitization approaches could achieve the visible light activity, the photocorrosion resistance and stability of these modified visible light active TiO_2 are often compromised because of the foreign elements introduced by doping and sensitization [16,23–27].

Rutile TiO_2 microspheres with exposed {1 1 1} facets were synthesized and used as UV light photocatalyst for bactericidal application [17]. In their study, the synthesized rutile TiO_2

* Corresponding author. Tel.: +61 7 55528261; fax: +61 7 55528067.
** Corresponding author. Tel.: +86 416 4673257.
E-mail addresses: chang.liu@vip.126.com (C. Liu), h.zhao@griffith.edu.au (H. Zhao).

0920-5861/$ – see front matter © 2013 Elsevier B.V. All rights reserved.
http://dx.doi.org/10.1016/j.cattod.2013.09.041

microspheres were filtrated by a cellulose acetate membrane to form a photocatalyst film. The inactivation experiments were carried out by adding 10 mL of *Staphylococcus Aureus* (1×10^4 CFU/ml) solution onto the photocatalyst film followed by UV treatment (main wavelength of 365 nm) for 2 h to achieve over 90% inactivation [17]. Recently, we and others successfully fabricated pure rutile TiO_2 with exposed {1 1 1} facets that possesses visible light activity [19,21,28]. An advantage of our synthetic approach [19,21] is that the rutile TiO_2 with 100% exposed {1 1 1} faceted pyramid-shaped surface can be directly grown onto FTO conducting substrate and used as the photoanode. This enables the use of electrochemical technique to overcome the drawback of unfavourable conduction band position of rutile TiO_2, improving the photocatalytic efficiency [19,21]. The resultant rutile TiO_2 photoanode with 100% exposed {1 1 1} facets demonstrated excellent visible light activities towards the photoelectrocatalytic oxidation of organics and water [19,21]. The origin of the visible light activity of such {1 1 1} faceted rutile TiO_2 can be ascribed to Ti^{3+} doping in the bulk [19,21,28].

In this work, the bactericidal performance of the pure rutile TiO_2 photoanode with 100% exposed {1 1 1} facets was investigated by photocatalytic and photoelectrocatalytic inactivation of *Escherichia coli* under both UV and visible light illumination. To the best of our knowledge, this is the first time the visible light bactericidal effect of a pure rutile TiO_2 photoanode is investigated. The photocatalytic inactivation performance under sunlight was also evaluated.

2. Experimental

2.1. Synthesis of rutile TiO_2 photoanode

The pure rutile TiO_2 film with 100% exposed pyramid-shaped {1 1 1} facets was directly grown onto a FTO conducting substrate by a facile hydrothermal method as previous described [19,21]. Briefly, 0.04 g of TiN (Sigma–Aldrich, >95%) was added to a mixture of 13.5 mL of deionized water (Millipore Corp., 18 MΩ cm), 13.5 mL of HCl (Sigma–Aldrich, 32%) and 3.0 mL of H_2O_2 (Sigma–Aldrich, 30%). After magnetically stirring for 60 s, the reaction solution was transferred into a Teflon-lined stainless steel autoclave (100 mL in volume). A piece of clean FTO conducting substrate (30 mm × 30 mm × 2 mm) was then immersed into the reaction solution with the conductive side facing up. The hydrothermal reaction was carried out at 200 °C for 24 h. After hydrothermal reaction, the autoclave was naturally cooled down to room temperature. The FTO substrate was taken out, rinsed adequately with deionized water and dried in a nitrogen stream. The resulting products were further calcined in a tube furnace at 450 °C for 2 h in argon (Ar) with a heating rate of 5 °C/min, and used as the photoanode.

2.2. Characterizations

The crystal structure of the sample was investigated by X-ray diffraction (XRD, Shimadzu XRD-6000, equipped with graphite monochromated Cu Kα radiation). Morphological information was collected by scanning electron microscopy (SEM, JSM-6300F).

2.3. Preparation of bacterial cells

A single colony of *E. coli* K12 (Southern Biological) grown on nutrient agar (NA, Oxoid) was removed using a pre-sterilized bacterial swab and inoculated into nutrient broth (NB, Oxoid). Incubated overnight at 37 °C with constant agitation under aerobic conditions, bacterial cells were harvested by centrifugation at 3000 rpm for 15 min. The bacterial pellet was resuspended in sterile deionized water, washing three times to eliminate residual organic and inorganic substances. The washed bacterial cells were resuspended in sterile deionized water and were diluted with 0.10 M $NaNO_3$ solution to obtain a concentration of *ca.* 1.0×10^7 CFU/mL.

2.4. Bactericidal performance

Both photocatalytic (PC) and photoelectrocatalytic (PEC) inactivation experiments under UV and visible light irradiation were carried out in a bulk cell with a quartz window for illumination, respectively (see Fig. 1). 45 mL of solution containing 0.10 M $NaNO_3$ and *ca.* 1.0×10^7 CFU/mL *E. coli* was placed in the reactor. For PC inactivation experiment, the fabricated rutile TiO_2 film on FTO substrate was fixed in the reactor. For PEC inactivation experiment, a three-electrode mode was applied, using the fabricated rutile TiO_2 film as photoanode, a saturated Ag/AgCl as reference electrode and a platinum mesh as counter electrode. A voltammograph (CV-27, BAS) was used for the application of potential bias, and a Macintosh (AD Instruments) was used to record the potential and current signals. A 150 W xenon arc lamp with focusing lenses (HF-200W-95, Beijing Optical Instruments) was used as light source. A UV-bandpass filter and a UV-400 filter (UG 5, Avotronics Pty. Ltd.) were used to obtain UV and visible light, respectively. The incident light intensity was fixed at 6.6 mW/cm^2 (main wavelength of 365 nm) for UV inactivation, and 150 mW/cm^2 (wavelength >400 nm) for visible light inactivation.

At regular time interval, 100 μL of solution was withdrawn and immediately serially diluted (10^{-1}, 10^{-2}, 10^{-3}, 10^{-4} and 10^{-5}) with sterile 0.9% NaCl solution (saline) to obtain between 20 and 200 colony forming units (CFUs) per plate. Subsequently, a collected sample (100 μL) was spread on nutrient agar plates and incubated at 37 °C in the dark for 20 ± 2 h. The developed colonies were enumerated and the number of viable cells was recorded in terms of CFU per unit volume of the reaction mixture. It should be noted that the data shown in this work were the average values of data obtained from experiments replicated in triplicate. For comparison, direct photolysis (using UV and visible light, respectively) and direct electrolytic inactivation experiments were also carried out;

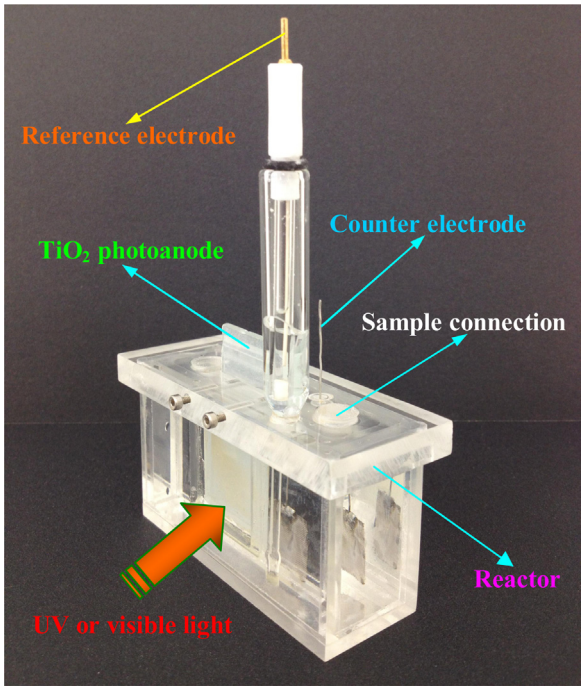

Fig. 1. Schematic illustration of home-made reactor for photocatalytically and photoelectrocatalytically bactericidal applications.

the former was conducted in the absence of photoanode under UV or visible light irradiation, while the latter was performed using the three-electrode system but in the absence of light irradiation.

The sunlight photocatalytic inactivation was performed. Typically, the fabricated rutile TiO_2 film was placed in a holder face-up, and 1.0 mL of *E. coli* solution (1.0×10^7 CFU/mL) was spread on the surface of the TiO_2 film in the holder and treated by the simulated sunlight with a light intensity of 100 mW/cm^2. After treatment, a 100 μL of treated solution was taken from photocatalyst film surface, and then spread on nutrient agar plates and incubated at 37 °C in the dark for 20 ± 2 h for further evaluation. The survival (%) of *E. coli* cells after light irradiation is calculated based on the following equation:

$$\text{Survival}\,(\%) = \frac{\text{CFU}}{\text{CFU}_0} \times 100(\%)$$

where, CFU_0 is the initial concentration of *E. coli* (1×10^7 CFU/mL). CFU is the concentration of alive *E. coli* cells with different light irradiation time.

3. Results and discussion

3.1. Structural characteristics

After calcination at 200 °C for 24 h in Ar, the fabricated product exhibits a tetragonal structured rutile phase TiO_2 (Fig. 2A), similar to those reported by us and other group [19,21,28]. Fig. 2B shows the surface and cross-sectional SEM images of the fabricated rutile TiO_2 film sample. As shown, the film displays a 100% exposed pyramid-shaped surface structure, and our previous works have confirmed that such exposed crystal facets are {1 1 1} facets [19,21]. Further, the fabricated rutile TiO_2 film has a thickness of *ca.* 4.9 μm (inset in Fig. 2B). The theoretical calculations results reported in our previous work have indicated that the exposed {1 1 1} faceted surface of the rutile TiO_2 film is a high energy surface with a surface energy of 1.46 J/m^2, much higher than that of the most stable {1 1 0} faceted surface of rutile TiO_2 (0.35 J/m^2) [19]. It has been recognized that the crystal facets with high surface energy usually possess high reactivity under light irradiation, favourable for catalytic oxidation processes [29–31]. Therefore, the exposed high energy {1 1 1} faceted surface of the fabricated rutile TiO_2 film could be of beneficial to improve the bactericidal performance. Importantly, previous studies have indicated that the fabricated rutile TiO_2 film possesses a narrowed bandgap (*ca.* 2.96 eV) compared to the commercially available P25 photocatalyst, meaning a capability of absorbing visible light [19,21]. The origin of the visible light activity of the pure rutile TiO_2 can be attributed to Ti^{3+} doping in the bulk [4,19,21,28]. Further experimental evidences have proven that the pure rutile TiO_2 film possesses excellent UV and visible light activities towards photocatalytic oxidation of water and organics [19,21].

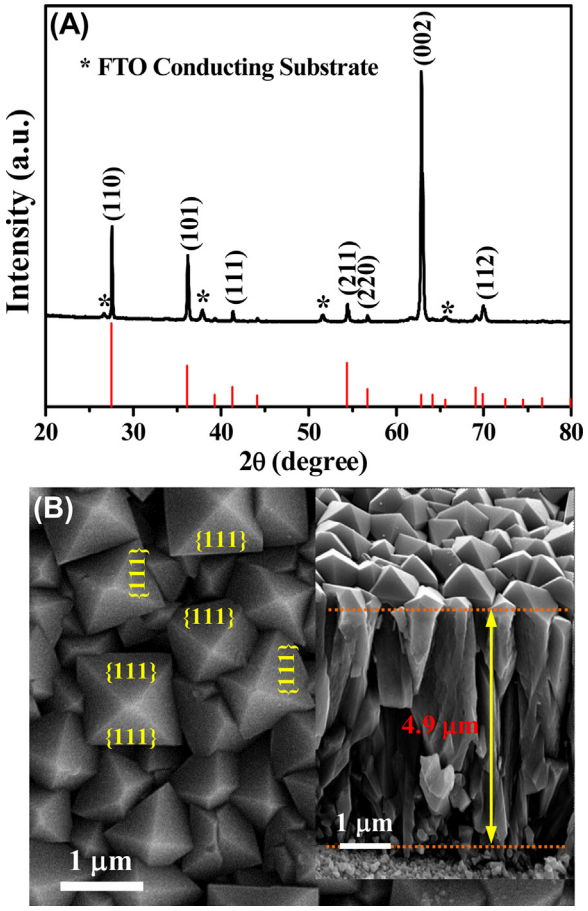

Fig. 2. (A) XRD patterns of the TiO_2 product calcined at 450 °C in Ar; (B) surface and cross-sectional (inset) SEM images of the TiO_2 sample calcined at 450 °C in Ar.

3.2. Photoelectrocatalytic activity

The photoelectrocatalytic activity of the rutile TiO_2 films under UV and visible light irradiation are firstly investigated. Fig. 3A and B shows the voltammograms of the rutile TiO_2 photoanodes obtained from 0.10 M $NaNO_3$ supporting electrolyte with or without light irradiation. It can be seen that without irradiation, only negligible currents can be measured (red curves in Fig. 3A and B). The obvious photocurrent responses can be generated when the photoanode is under UV or visible light illumination (black curves in Fig. 3A and B). The obtained photocurrent responses are resulted from the photocatalytic oxidation of water, confirming that the photoanode is photoactive under both UV and visible light. The measured photocurrents increase initially with the applied potential bias and reach saturated status at higher potentials. The critical potentials for the photocurrents to achieve saturation (+0.31 and + 0.30 V for UV and visible light illumination, respectively) are corresponding to the bottom edge of the conduction band [19,21]. In theory, 100% of photogenerated electrons should be removed from the conduction band when the applied potential is more positive than that of the critical potential. Considering possible potential drops caused by other factors, an applied potential bias of + 0.40 V is chosen in this work for subsequently photoelectrocatalytic bactericidal experiments. Fig. 3C and D shows the transient photocurrent responses obtained from a solution containing 0.10 M $NaNO_3$ electrolyte with a + 0.40 V applied potential bias under different intensities of UV and visible light illuminations. Apparently, the measured photocurrents under both UV and visible light irradiation are proportionally increased with the increased light intensities, confirming that the +0.40 V applied potential bias is sufficient.

3.3. Bactericidal performance under UV irradiation

Fig. 4 shows the inactivation data of *E. coli* cells under different conditions. As shown, the survival ratio of *E. coli* cells is not affected by the direct electrolysis at +0.40 V, indicating that an applied potential bias of +0.40 V applied potential cannot directly inactivate *E. coli* cells *via* electrolysis. In the absence of rutile TiO_2 photocatalyst, a direct photolysis under UV irradiation results in an 8.73% inactivation with 30 min of irradiation. However, in the presence of rutile TiO_2 film (photoanode), an inactivation percentage of 66.03% can be reached within 10 min of UV irradiation. A 96.43% inactivation can be achieved within 30 min of UV irradiation. The

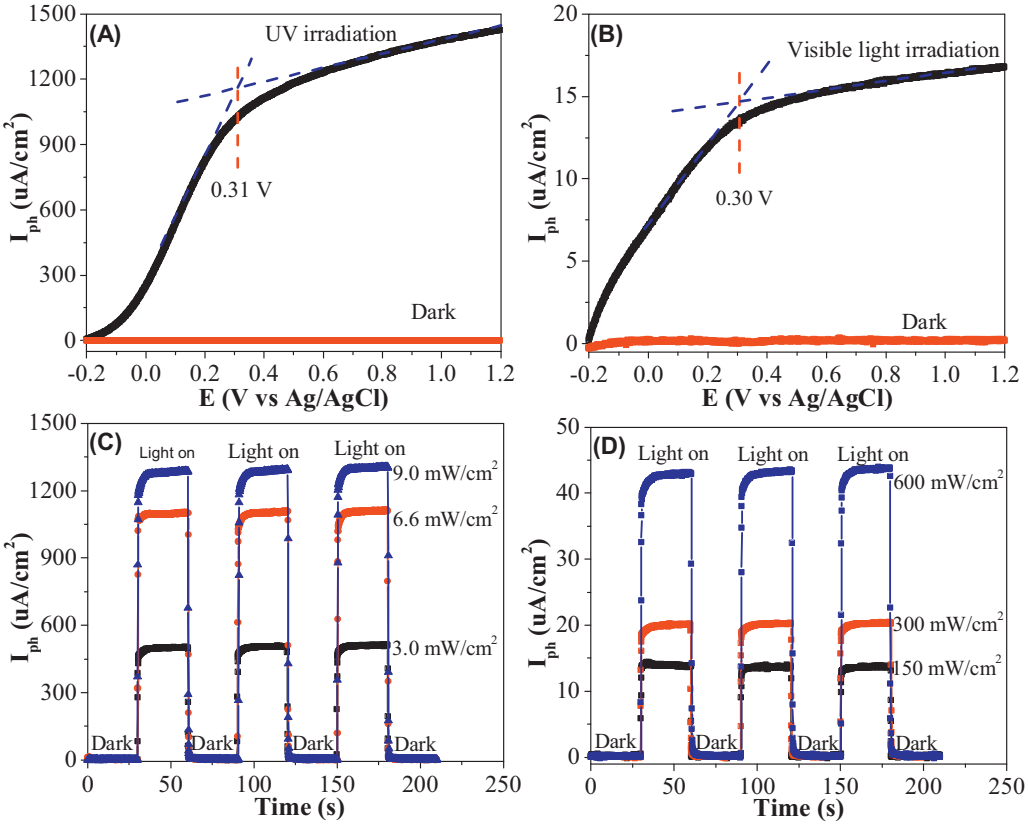

Fig. 3. (A) and (B) Voltammograms obtained from the rutile TiO_2 photoanode in 0.10 M $NaNO_3$ supporting electrolyte under UV and visible light irradiation, respectively. UV light intensity of 6.6 mW/cm^2 and visible light intensity of 150 mW/cm^2. Transient photocurrent responses obtained at +0.40 V applied potential bias under UV (C) and visible light (D) irradiation with different light intensities, respectively. (For interpretation of the references to colour in the text, the reader is referred to the web version of the article.)

improved inactivation efficiency can be attributed to the bactericidal effect of the rutile TiO_2 photocatalysis under UV irradiation. The inactivation efficiency is remarkably enhanced with photoelectrocatalytic treatment. A 95.24% inactivation can be obtained with only 5 min of photoelectrocatalytic treatment. Almost 100% of *E. coli* can be inactivated after 10 min of photoelectrocatalytic treatment. It is generally agreed that the bactericidal effect of the TiO_2 photocatalysis-based techniques is achieved *via* the photocatalytically generated active oxygen species (AOSs) such as $^{\bullet}OH$, $H_2O^{\bullet}$, O_2^- [12,32]. The dramatically enhanced bactericidal performance by photoelectrocatalysis can be attributed to the effectively suppressing the charge recombination, enabling the production of high concentrations AOSs that act as the bactericides for fast killing [12,32]. The photogenerated holes at the valence band of TiO_2 are a more powerful oxidant (bactericide) than that of AOSs [12,18]. The photogenerated holes could directly act as a bactericide with a photoelectrocatalytic system due to their prolonged lifetimes, which could be another attribute for the enhanced bactericidal performance [11,12]. Further, under the given experimental conditions, the photocatalytic and photoelectrocatalytic inactivation of *E. coli* cells are of first order reactions. The calculated inactivation kinetic constants (k) are 0.0513 and 0.2691 min^{-1} for photocatalysis and photoelectrocatalysis, respectively (Table 1), indicating that the photoelectrocatalytic inactivation efficiency is over 5 times of that photocatalysis.

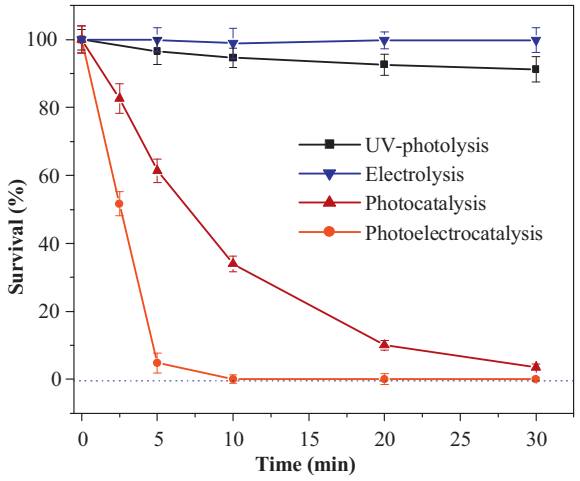

Fig. 4. Survival of *E. coli* cells with time by UV-photolysis, electrolysis, photocatalysis, and photoelectrocatalysis. The concentration of *E. coli* is 1×10^7 CFU/mL; UV light intensity of 6.6 mW/cm^2, applied potential bias of +0.40 V.

3.4. Bactericidal performance under visible light and sunlight irradiation

All bactericidal experiments were carried out use the same photoelectrochemical reactor as used for UV bactericidal experiments

Table 1
First order reaction kinetic constants of photocatalytically and photoelectrocatalytically bactericidal reactions using rutile TiO_2 films under UV and visible light irradiation.

Light source	Photocatalysis k (min^{-1})	Photoelectrocatalysis k (min^{-1})
UV	0.0513	0.2691
Visible light	0.0046	0.0159

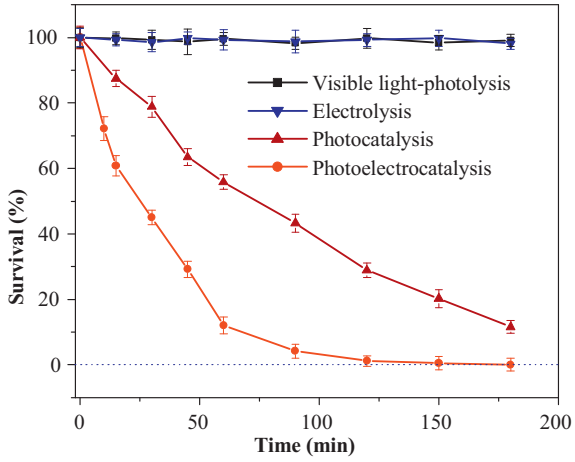

Fig. 5. Survival of *E. coli* cells with time by visible light-photolysis, electrolysis, photocatalysis, and photoelectrocatalysis. The concentration of *E. coli* is 1×10^7 CFU/mL, visible light intensity of 150 mW/cm^2, applied potential bias of +0.40 V.

(Fig. 1). The experimental conditions were the same as the corresponding UV bactericidal experiment, except a visible light source was used to replace the UV light source. Fig. 5 shows the inactivation of *E. coli* cells under visible light irradiation. The direct electrolysis with an application of +0.40 V shows no measurable effect on the survival of *E. coli* cells, indicating the inability to inactivate *E. coli* cells under the experimental conditions. Differing from the case of direct UV-photolysis, no noticeable bactericidal effect can be measured with direct visible light-photolysis treatment due to the low photon energy of visible light that is unable to cause damage to *E. coli* cells. The photocatalysis treatment in the presence of the rutile TiO_2 photocatalyst film can lead to the inactivation of *E. coli* cells. 88.46% of *E. coli* cells can be inactivated after 180 min of photocatalytic treatment. For photoelectrocatalysis, 87.92% inactivation can be reached within 60 min of treatment and a prolonged treatment time of 180 min results in a complete inactivation of 1×10^7 CFU/mL *E. coli* cells. The improved bactericidal performance under photoelectrocatalytic conditions are due to the similar reasons as described for the UV driven photoelectrocatalysis bactericidal process [12,32]. Same to the case of UV treatment, the inactivation kinetics under visible light with photocatalysis and photoelectrocatalysis treatments are also the first order reaction. The calculated k values are 0.0046 and 0.0159 min^{-1} for photocatalysis and photoelectrocatalysis, respectively (Table 1), indicating that the visible light photoelectrocatalysis treatment is nearly 3.5 times more effective than that of photocatalysis under the same conditions. It can be seen from Table 1 that the k value of UV-photocatalysis is over 11 times of the visible light photocatalysis, while the k value of UV-photoelectrocatalysis is nearly 17 times of the visible light photoelectrocatalysis.

The photocatalytic bactericidal performance of the rutile TiO_2 film under sunlight was also evaluated in this work. Simulated sunlight with a light intensity of 100 mW/cm^2 was used. As shown in Fig. 6A, no survival *E. coli* cell can be observed within 2.0 min of sunlight irradiation. A detailed investigation reveals that sunlight photocatalytic treatment can achieve 83.19% and 96.26% inactivation within 1.0 and 1.5 min (Fig. 6B), respectively. Within 1.9 min of sunlight irradiation, 99.97% inactivation can be reached and a complete inactivation can be readily achieved within 2.0 min of sunlight photocatalysis treatment. It is well-known that some visible light photocatalysts such as Cu_2O and CdS are unstable under sunlight because the presence of UV irradiation, limiting their applications [16,33]. As demonstrated in the earlier part of this work, the visible light active {1 1 1} faceted rutile TiO_2 film used here is stable under UV light irradiation [19]. The reusability of the rutile TiO_2 film for the sunlight-driven photocatalytic inactivation of *E. coli* cells was evaluated by a 20 successive inactivation experiments (Fig. 6C). No noticeable bactericidal performance change was observed, demonstrating a superior stability.

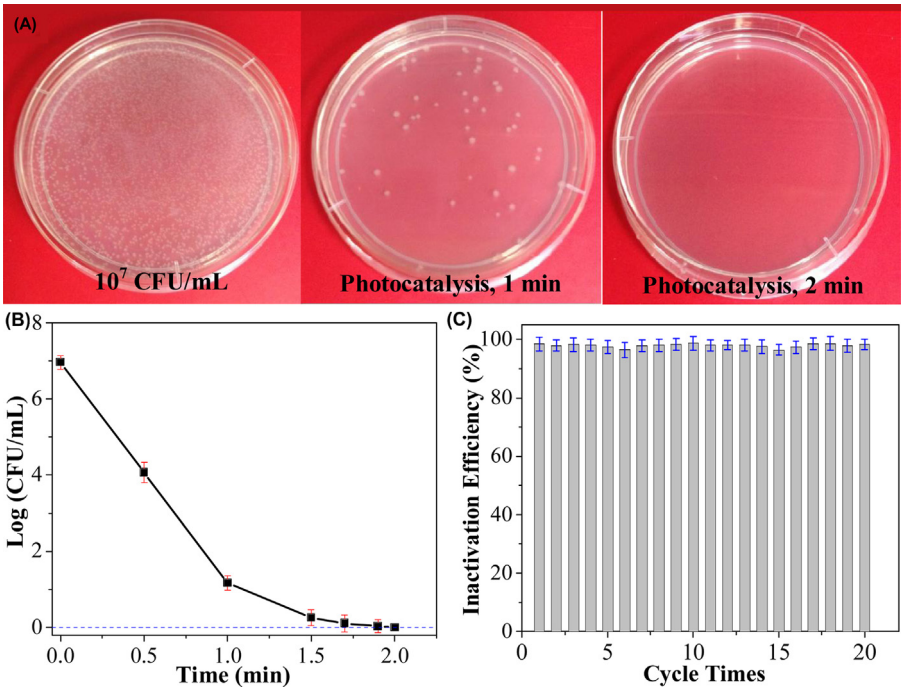

Fig. 6. (A) Photographs of survival of *E. coli* cells with time by direct photocatalysis using simulated solar light source with light intensity of 100 mW/cm^2. (B) Survival of *E. coli* cells with time by photocatalysis under sunlight irradiation. (C) Bactericidal stability of rutile TiO_2 film by photocatalysis under sunlight irradiation. The concentration of *E. coli* is 1×10^7 CFU/mL and the light irradiation time is 1.7 min.

4. Conclusion

The fabricated rutile TiO_2 photoanode with 100% exposed high energy {1 1 1} faceted surface is photoactive under both UV and visible light irradiation and exhibits excellent bactericidal performance with UV and visible light driven photocatalytic and photoelectrocatalytic treatments. The experimental results confirm the superiority of the photoelectrocatalysis over the photocatalysis for bactericidal application. The photoelectrocatalytic inactivation efficiencies are found to be 5 and 3.5 times of that photocatalysis under UV and visible light irradiation. The reported photoanode is highly stable, enabling the direct utilization of sunlight to drive the photocatalytic bactericidal process.

Acknowledgements

This work was supported financially by Australia Research Council (ARC) Discovery Project and Department of Education, Liaoning Provincial Government, China (L2011152).

References

[1] F. Huang, D. Chen, X.L. Zhang, R.A. Caruso, Y.-B. Cheng, Adv. Funct. Mater. 20 (2010) 1301.
[2] A. Fujishima, X. Zhang, D.A. Tryk, Surf. Sci. Rep. 63 (2008) 515.
[3] G.K. Mor, K. Shankar, M. Paulose, O.K. Varghese, C.A. Grimes, Nano Lett. 5 (2005) 191.
[4] F. Zuo, L. Wang, T. Wu, Z. Zhang, D. Borchardt, P. Feng, J. Am. Chem. Soc. 132 (2010) 11856.
[5] M.R. Hoffmann, S.T. Martin, W. Choi, D.W. Bahnemann, Chem. Rev. 95 (1995) 69.
[6] A. Hagfeldt, M. Graetzel, Chem. Rev. 95 (1995) 49.
[7] H. Zhao, D. Jiang, S. Zhang, W. Wen, J. Catal. 250 (2007) 102.
[8] D. Jiang, S. Zhang, H. Zhao, Environ. Sci. Technol. 41 (2007) 303.
[9] P.A. Christensen, T.P. Curtis, T.A. Egerton, S.A.M. Kosa, J.R. Tinlin, Appl. Catal. B 41 (2003) 371.
[10] C. McCullagh, J.C. Robertson, D. Bahnemann, P.J. Robertson, Res. Chem. Intermed. 33 (2007) 359.
[11] P.-C. Maness, S. Smolinski, D.M. Blake, Z. Huang, E.J. Wolfrum, W.A. Jacoby, Appl. Environ. Microbiol. 65 (1999) 4094.
[12] G. Li, X. Liu, H. Zhang, T. An, S. Zhang, A.R. Carroll, H. Zhao, J. Catal. 277 (2011) 88.
[13] T. Matsunaga, R. Tomoda, T. Nakajima, H. Wake, FEMS Microbiol. Lett. 29 (1985) 211.
[14] P.S.M. Dunlop, J.A. Byrne, N. Manga, B.R. Eggins, J. Photochem. Photobiol. A 148 (2002) 355.
[15] F. Rahmawati, T. Kusumaningsih, A. Hastuti, Toxicol. Environ. Chem. 93 (2011) 1602.
[16] S. Zhang, C. Liu, X. Liu, H. Zhang, P. Liu, S. Zhang, F. Peng, H. Zhao, Appl. Microbiol. Biotechnol. 96 (2012) 1201.
[17] L. Sun, Y. Qin, Q. Cao, B. Hu, Z. Huang, L. Ye, X. Tang, Chem. Commun. 47 (2011) 12628.
[18] D. Jiang, H. Zhao, S. Zhang, R. John, J. Phys. Chem. B 107 (2003) 12774.
[19] H. Zhang, X. Liu, Y. Wang, P. Liu, W. Cai, G. Zhu, H. Yang, H. Zhao, J. Mater. Chem. A 1 (2013) 2646.
[20] H. Zhang, X. Liu, Y. Li, Q. Sun, Y. Wang, B.J. Wood, P. Liu, D. Yang, H. Zhao, J. Mater. Chem. 22 (2012) 2465.
[21] X. Liu, H. Zhang, X. Yao, T. An, P. Liu, Y. Wang, F. Peng, A. Carroll, H. Zhao, Nano Res. 5 (2012) 762.
[22] H. Zhang, H. Zhao, S. Zhang, X. Quan, ChemPhysChem 9 (2008) 117.
[23] Y. Hou, X. Li, Q. Zhao, G. Chen, C.L. Raston, Environ. Sci. Technol. 46 (2012) 4042.
[24] F.-J. Zhang, M.-L. Chen, W.-C. Oh, Compos. Sci. Technol. 71 (2011) 658.
[25] S.C. Hayden, N.K. Allam, M.A. El-Sayed, J. Am. Chem. Soc. 132 (2010) 14406.
[26] G. Liu, L. Wang, H.G. Yang, H.-M. Cheng, G.Q. Lu, J. Mater. Chem. 20 (2010) 831.
[27] G. Liu, G. Yang Hua, X. Wang, L. Cheng, J. Pan, M. Lu Gao Qing, H.-M. Cheng, J. Am. Chem. Soc. 131 (2009) 12868.
[28] F. Zuo, K. Bozhilov, R.J. Dillon, L. Wang, P. Smith, X. Zhao, C. Bardeen, P. Feng, Angew. Chem. Int. 51 (2012) 6223.
[29] H.G. Yang, C.H. Sun, S.Z. Qiao, J. Zou, G. Liu, S.C. Smith, H.M. Cheng, G.Q. Lu, Nature 453 (2008) 638.
[30] H. Zhang, P. Liu, F. Li, H. Liu, Y. Wang, S. Zhang, M. Guo, H. Cheng, H. Zhao, Chem. Eur. J. 17 (2011) 5949.
[31] H. Zhang, Y. Wang, P. Liu, Y. Han, X. Yao, J. Zou, M. Cheng Hui, H. Zhao, ACS Appl. Mater. Interf. 3 (2011) 2472.
[32] M. Cho, H. Chung, W. Choi, J. Yoon, Water Res. 38 (2004) 1069.
[33] D.R. Baker, P.V. Kamat, Adv. Funct. Mater. 19 (2009) 805.